Automatic detection of endobronchial lesions with virtual bronchoscopy: comparison of two methods

Ronald M. Summers* , Lynne M. Pusanik, and James D. Malley

Diagnostic Radiology Department, Warren Grant Magnuson Clinical Center
National Institutes of Health, Bethesda, MD 20892-1182

ABSTRACT

Three-dimensional reconstruction of medical images is increasingly being used to diagnose disease and to direct therapy. Virtual bronchoscopy is a recently developed type of three-dimensional reconstruction of the airways that may be useful for diagnosis of lesions of the airway. In this study, we compare two methods for computer-aided diagnosis of polypoid airway tumors: a parametric ("patch") and non-parametric ("grey-scale") algorithm. We found that both methods have comparable specificities. Although the non-parametric method is twelve times faster than the parametric method, we found that its sensitivity lags behind that of the parametric method by 3 to 16% when lesions of all sizes are considered. For lesions at least 5 mm in size, the sensitivities are comparable if a small convolution kernel is used.

Keywords: computed tomography; virtual bronchoscopy; computer-aided diagnosis; bronchi; trachea; curvature; three-dimensional reconstruction

1. INTRODUCTION

Virtual bronchoscopy is a new method of displaying three-dimensional reconstructions of the central airways. It produces an endoscope-like display that has proved accurate for the assessment of stenoses and masses affecting the airways [1-4].

Curvature based segmentation methods have been previously applied to range images and medical imaging for computer vision and object registration [5,6]. We have tested two methods of image analysis based on curvature segmentation to compare their usefulness for another application: computer-assisted detection of endobronchial lesions on virtual bronchoscopy studies.

We have previously reported on a patch-based method for automatic lesion detection [7]. That method, based on parameterization of the airway surface, yielded high sensitivities and specificities for detecting lesions. However, it had two limitations: it ran slowly and worked poorly in the smallest airways. Both of these limitations were a direct consequence of the need to parameterize the surface using b-spline patches. In this report we compare the patch-based method with a faster nonparametric method based on computing curvatures directly from the grey-scale data.

2. METHODS

Virtual bronchoscopy (VB) three-dimensional surface renderings of the central airways were generated from computed tomography (CT) scans of the thorax in 7 patients with and 9 patients without endobronchial lesions [4,8]. A latex airway phantom fitted with simulated endobronchial lesions was also scanned [9]. Automatic detection of the lesions was done using two curvature-based techniques: one which determined local curvature over small patches on the surface (hereinafter referred to as the "patch" algorithm) and another which computed curvature from the underlying grey-scale data (the "grey-scale" algorithm). Each method uses the local curvature to detect the presence of a curvature signature characteristic of a lesion and color encodes the surface at that location. We performed quantitative analyses of these color-encoded surfaces in order to determine the sensitivity and specificity of lesion detection for the two methods, using the original CT scan data as the gold standard. We also analyzed the color-encoded surfaces to ascertain qualitative differences between the two methods.

* Send correspondence to R.M.S.
E-mail: rms@nih.gov

The CT images were first pre-processed using a seeded region-growing algorithm in order to identify the airways [4]. The region-growing algorithm identified a thin shell of voxels surrounding the lumen which were designated as the airway wall. A shell two voxels thick was used for the surface patch method to which a standard isosurface tessellation algorithm was applied and an OpenInventor scene graph was produced [10,11].

For the patch method, the surface was first smoothed and then overlapping 5 mm bicubic parametric B-spline patches were fit to each point of the surface using least squares [5,7,12-14]. The differential characteristics of the surface (i.e., its local curvature) at each vertex could then be computed from first and second order partial derivatives of the B-spline patch [5,7,13-15]. These curvatures were then classified as elliptical, hyperbolic, or cylindrical curvature based on the signs of the principal curvatures. Potential polypoid lesions were designated as those having elliptical curvature of the peak subtype. To reduce the number of false positive detections, a connectivity algorithm was applied to further refine the list of potential lesion sites.

For the grey-scale method, 3D filters to compute partial derivatives of the image data were formed [16,17]. The size of the 3D filters was set to approximately 5x5x5 mm^3 with an adjustment made for the anisotropy of the 3D dataset. For example, a kernel of size 11x11x11 voxels actually used an 11x11 voxel component in the plane of section (0.5 mm in-plane voxel size) but along the longitudinal direction (1 mm section thickness) the kernel was only 5 voxels thick. The normalization coefficients of these filters were computed using discrete sums performed over the size of the kernel. The separable filters were then applied to the image I(x,y,z) using convolutions to compute smoothed partial derivatives. These partial derivatives were used to compute the Gaussian (K), mean (H), and principal curvatures (κ_{MIN}, κ_{MAX}) at each vertex on the isosurface. The curvature values were used to colorize the surface based on various selection criteria (type of curvature, range of values, connectivity of neighboring vertices of like curvature classification).

For both methods of curvature computation, the following minimum criteria were used to classify a lesion: curvature classification of the "peak" subtype and minimum lesion size 30 vertices (approximately 3 mm). Three thresholds (ε) for mean or maximum principal curvature were used: $\varepsilon < 0$, $\varepsilon < -1$, $\varepsilon < -2$. The number of potential lesion sites meeting these criteria were counted and were individually evaluated for plausibility using a multiple window 3D surface geometry viewer and an airway navigation software tool [8,18]. The color-encoded surfaces can also be evaluated with any VRML 1.0-compliant viewer. Processing and display were done on an Onyx2 Infinite Reality workstation (Silicon Graphics, Inc.) having 512 MB main memory and using a single 195 MHz R10000 processor.

Sensitivity and specificity for each mean curvature threshold were reported on a per segment basis for statistical purposes. There were five airway segments: trachea, right and left mainstem bronchus, and right and left lung lobar and segmental bronchi. Data for the patch method were reported elsewhere and are included here for comparison [19].

3. RESULTS

Both methods detected all simulated endobronchial lesions at least 5 mm in size in the phantom (Figure 1 and Figure 2). None of the simulated lesions smaller than 5 mm was detected with either method except for one case in which a 4 mm lesion was detected (grey-scale method, 7x7x9 voxel kernel).

When lesions of all sizes were considered, the sensitivity of the patch method was better than that of the grey-scale method although the specificities were similar (Table 1). The sensitivity of the grey-scale method improved 5 - 16% using a smaller kernel, with a similar specificity (Table 1 and Figure 3). When only lesions at least 5 mm in size were considered, the sensitivities improved up to 28% for the grey-scale method.

For the patient studies, the number of lesion detections found and subsequently discarded at sites of segmentation leakage, end effects (an artifactual cap at the distal extent of a segmental airway), or artifacts from poor segmentation, was approximately 25 per patient with the grey-scale method and 2 per patient with the patch method.

The grey-scale method was more computationally efficient, requiring only 9% of the processing time required by the surface based method. Per thousand triangles, isosurface generation took 0.2 sec, and curvature computation took 1.2 sec (grey-scale method, 11x11x11 kernel) or 13.5 sec (patch method). For the grey-scale method, smaller kernels required

significantly less processing time. For example, the 7x7x9 kernel executed at 0.5 sec per thousand triangles, over twice as fast as the 11x11x11 kernel.

The type of curvature used was also important. Using the mean curvature (H) with the grey-scale method, there were two to three times as many lesion detections for $\varepsilon < -1$ and $\varepsilon < -2$ compared to processing which used the maximum curvature (κ_{MAX}).

Qualitatively, the grey-scale method produced more visually appealing color-encoded surfaces because potential lesions were painted more homogeneously. In addition, the grey-scale method combined smoothing, isosurface generation, and lesion detection into one step whereas the surface based method required a series of steps. The problem of parameterizing the surface, often difficult or impossible in regions that were highly curved, is also avoided by using the grey-scale data. Also, the surface itself was not smoothed, so the model is closer to the actual data. Characteristics of the patch and grey-scale methods are compared and contrasted in Table 3.

4. DISCUSSION

We found that the grey-scale method had slightly lower sensitivity than the patch method, even when a smaller kernel which yielded better sensitivity was used. We believe the smaller kernel was advantageous because the larger kernel may smooth the airway wall to a greater extent because of contributions of non-airway structures further from the airway wall. We also note that the kernels have adjustable parameters (α in the 3D Deriche filters in Ref. 16) which affect the degree of smoothing.

The grey-scale method was twelve times as fast as the patch method. This is because parameterization of the surface was computationally expensive. However, both methods are amenable to parallelism and the number of computations required are linear in the number of vertices in the airway surface. The 3D filter kernel is fast because it only needs to be applied at each vertex. The convolution does not need to be applied to the entire dataset which would scale with the size of the dataset. Methods now exist for accelerating convolutions in special purpose hardware which could be used to make the grey-scale method faster yet. Use of a smaller kernel would make the grey-scale method over 24 times as fast as the patch method, potentially increasing sensitivity at the same time.

Although the grey-scale method should work better than the patch method in smaller airways where the curvature is greater, our results for the airway phantom showed little difference between the two methods although the grey-scale method did detect one 4 mm lesion in the phantom which the patch method missed. However, our choice of connected component size (30 vertices) may have caused us to discard such detections. The same limitation applied to our analysis of the patient studies. Further work will need to be done to determine if detection of lesions in the small airways can be achieved without generation of a significant number of false positive detections.

These lesion detection methods could also be applied to virtual endoscopy systems which only render local anatomy, for example those which do not try to generate the entire exoscopic view but only compute endoscopic views based on the small range of structures visible at any one time during endoscopy. Such systems have gained favor because they do not require a difficult segmentation to be performed and they require less or no pre-processing. For such an application, the airway wall could be colorized and the presence of potential lesions indicated as the physician navigates the particular segment of the hollow anatomic structure. The system would be unable to indicate all potential lesions up front because no global 3D anatomic model had been computed.

In this project, we used an anisotropic kernel to match the anisotropy of the dataset. Another approach would be to interpolate the grey-scale data in order to obtain an isotropic dataset. If interpolation were done, the speed advantage of the grey-scale method would be reduced somewhat.

These are preliminary data based on one rational choice of parameters. However, as can be seen in Table 3, there are a multitude of possible parameter choices, some combination of which may yield improved sensitivity and specificity for lesion detection.

In conclusion, the grey-scale based lesion detection method is more computationally efficient, is amenable to parallelism, and produces more pleasing displays without compromising specificity. Its sensitivity is slightly lower

however, although sensitivity is improved by reducing the size of the kernel. The significance of these methods is that they may improve physician efficiency and accuracy in the detection of endobronchial lesions which protrude into the lumen. They may also be applicable for detecting other endoluminal masses such as colonic polyps.

ACKNOWLEDGMENTS

We thank the CT technologists at the NIH Clinical Center for performing the patient scans, Dr. David Shaw for constructing the airway phantom, Dr. Andrew Dwyer for review of the manuscript, and Drs. Steve Holland, Michael Sneller, Carol Langford, and James Shelhamer for patient referral.

REFERENCES

1. D. J. Vining, K. Liu, R. H. Choplin and E. F. Haponik, "Virtual bronchoscopy: relationships of virtual reality endobronchial simulations to actual bronchoscopic findings," *Chest* **109**, pp. 549-553, 1996.
2. H. U. Kauczor, B. Wolcke, B. Fischer, P. Mildenberger, J. Lorenz and M. Thelen, "Three-dimensional helical CT of the tracheobronchial tree: evaluation of imaging protocols and assessment of suspected stenoses with bronchoscopic correlation," *Am J Roentgenol* **167**, pp. 419-24, 1996.
3. M. Lacrosse, J. P. Trigaux, B. E. Van Beers and P. Weynants, "3D spiral CT of the tracheobronchial tree," *J Comput Assist Tomogr* **19**, pp. 341-7, 1995.
4. R. M. Summers, D. F. Feng, S. M. Holland, M. C. Sneller and J. H. Shelhamer, "Virtual bronchoscopy: segmentation method for real time display," *Radiology* **200**, pp. 857-862, 1996.
5. P. J. Besl and R. C. Jain, "Segmentation through variable-order surface fitting," *IEEE Trans. Pattern Anal. Machine Intell.* **10**, pp. 167-192, 1988.
6. J.-P. Thirion, O. Monga, S. Benayou, A. Gueziec and N. Ayache, "Automatic registration of 3D images using surface curvature," *Mathematical methods in medical imaging* **1768**, pp. 206-216, SPIE, 1992.
7. R. M. Summers, W. S. Selbie, J. D. Malley, L. Pusanik, A. J. Dwyer, N. Courcoutsakis, D. E. Kleiner, M. C. Sneller, C. Langford and J. H. Shelhamer, "Computer-Assisted Detection of Endobronchial Lesions Using Virtual Bronchoscopy: Application of Concepts from Differential Geometry," *Conference on mathematical models in medical and health sciences*, Vanderbilt University, Nashville, TN, 1997.
8. R. M. Summers, "Navigational aids for real-time virtual bronchoscopy," *AJR* **168**, pp. 1165-70, 1997.
9. R. M. Summers, D. J. Shaw and J. H. Shelhamer, "CT Virtual bronchoscopy of simulated endobronchial lesions: effect of scanning, reconstruction, and display settings and potential pitfalls," *AJR* in press, 1998.
10. W. E. Lorensen and H. E. Cline, "Marching Cubes: A High Resolution 3D Surface Reconstruction Algorithm," *ACM Computer Graphics* **21**, pp. 163-169, 1987.
11. J. Wernecke, *The inventor mentor: Programming object oriented 3D graphics with Open Inventor, release 2*, Addison-Wesley, Reading, Mass., 1994.
12. G. Taubin, "A signal processing approach to fair surface design," *SIGGRAPH* pp. 351-358, ACM, Los Angeles, CA, 1995.
13. P. Dierckx, *Curve and surface fitting with splines*, Clarendon, Oxford, 1993.
14. D. F. Rogers and J. A. Adams, *Mathematical elements for computer graphics*, 2nd ed., McGraw-Hill, New York, 1990.
15. J. C. Dill, "An application of color graphics to the display of surface curvature," *Computer Graphics* **15**, pp. 153-161, 1981.
16. O. Monga and S. Benayoun, "Using partial derivatives of 3D images to extract typical surface features," *Comput Vision Image Understand* **61**, pp. 171-189, 1995.
17. J.-P. Thirion and A. Gourdon, "Computing the differential characteristics of isointensity surfaces," *Comput Vision Image Understand* **61**, pp. 190-202, 1995.
18. R. M. Summers, "Image gallery: a tool for rapid endobronchial lesion detection and display using virtual bronchoscopy," *Society for computer applications in radiology*, in press, SCAR, Baltimore, 1998.
19. R. M. Summers, W. S. Selbie, J. D. Malley, L. M. Pusanik, A. J. Dwyer, N. Courcoutsakis, D. J. Shaw, D. E. Kleiner, M. C. Sneller, C. A. Langford, S. M. Holland and J. H. Shelhamer, "Virtual bronchoscopy of airway lesions: computer-assisted detection of polypoid lesions using surface curvature," *submitted*.
20. P. J. Besl, *Surfaces in range image understanding*, Springer-Verlag, New York, 1988.

Table 1. Sensitivity and Specificity of Patch and Grey-scale Methods.

	Patch Algorithm*		Grey-scale Algorithm 11x11x11 Kernel		Grey-scale Algorithm 7x7x9 Kernel	
ε	Sensitivity	Specificity	Sensitivity	Specificity	Sensitivity	Specificity
All Lesions						
0	88%	58%	72%	63%	78%	64%
-1	88%	70%	67%	74%	72%	75%
-2	47%	89%	28%	88%	44%	83%
5 mm Lesions or Larger						
0	100%	59%	100%	63%	100%	63%
-1	100%	77%	91%	73%	100%	75%
-2	64%	89%	27%	86%	55%	82%

Sensitivity and specificity are reported for 90 airway segments in 18 virtual bronchoscopy patient examinations. ε is the threshold for mean curvature (cm^{-1}).
*From Ref. 19.

Table 2. Comparison of Patch and Grey-scale Methods

Characteristic	Patch Method	Grey-scale Method	Comments
Relative speed	Slow	Fast	Factor of 12 difference in computational speed
Detected size (coverage) of any given lesion	Larger for low curvature lesions; smaller for high curvature lesions	Smaller for low curvature lesions; larger for high curvature lesions	Smaller detected size can cause candidate lesion to be falsely rejected based on size criteria
Data requirements	Only the surface	Both the surface and grey-scale data	5 MB vs. 50 - 100 MB
Amenable to parallelism	Yes	Yes	Curvature at each vertex can be computed independently of the others
Requires parameterization	Yes	No	Parameterization may fail if patch is too large in regions of high curvature
Behavior in smallest airways	Algorithm fails; unable to compute patch (insufficient density of vertices in regions of high curvature)	Not a limitation	Triangle splitting may be used to increase density of vertices for patch method, although computation time will increase proportionately
Requires smoothing	Yes; both surface and curvatures are smoothed	Yes; derivatives only are smoothed	Can result in loss of information and decreased sensitivity, possibly to a greater extent with patch method. Original surface is left intact with grey-scale method
Appearance of detected lesion (uniformity of coverage)	Heterogeneous (less uniform)	Homogeneous (more uniform)	Homogeneous (more uniform) appearance is more visually appealing
Depends on kernel size	N/A	Yes	Detected lesion size can be dramatically different for different size kernels
Likelihood of false positive detections within areas of segmentation leakage	Less likely	More likely	Manual editing may be used to reduce segmentation leakage although such editing is time consuming and not yet amenable to automation

Table 3. Degrees of Freedom for Lesion Detection Algorithm

Parameter	Possible choices	Parameters we used
Curvature Type	Gaussian (K), Mean (H), Principal (κ_{MIN}, κ_{MAX})	K, κ_{MAX}
Secondary and Derived curvatures - see Ref. 20	metric determinant $\sqrt{g}$, quadratic variation Q, coordinate angle function Θ, magnitude of principal curvature difference $\sqrt{H^2 - K}$, HK-sign map	N/A
Filter settings for desirable curvature values	Arbitrary	Upper limit: 0, -1, or -2 cm^{-1} Lower limit: -20 cm^{-1}
Kernel size+	Arbitrary	7x7x9, 9x9x9, 11x11x11 voxels (~3, 4, 5 mm in each direction, resp.)
Connected component size (minimum region size having homogeneous curvature classification)	Arbitrary	30 vertices (~3 mm diameter)
Patch size*	Arbitrary	5 mm

+Applies to grey-scale method only. *Applies to patch method only.

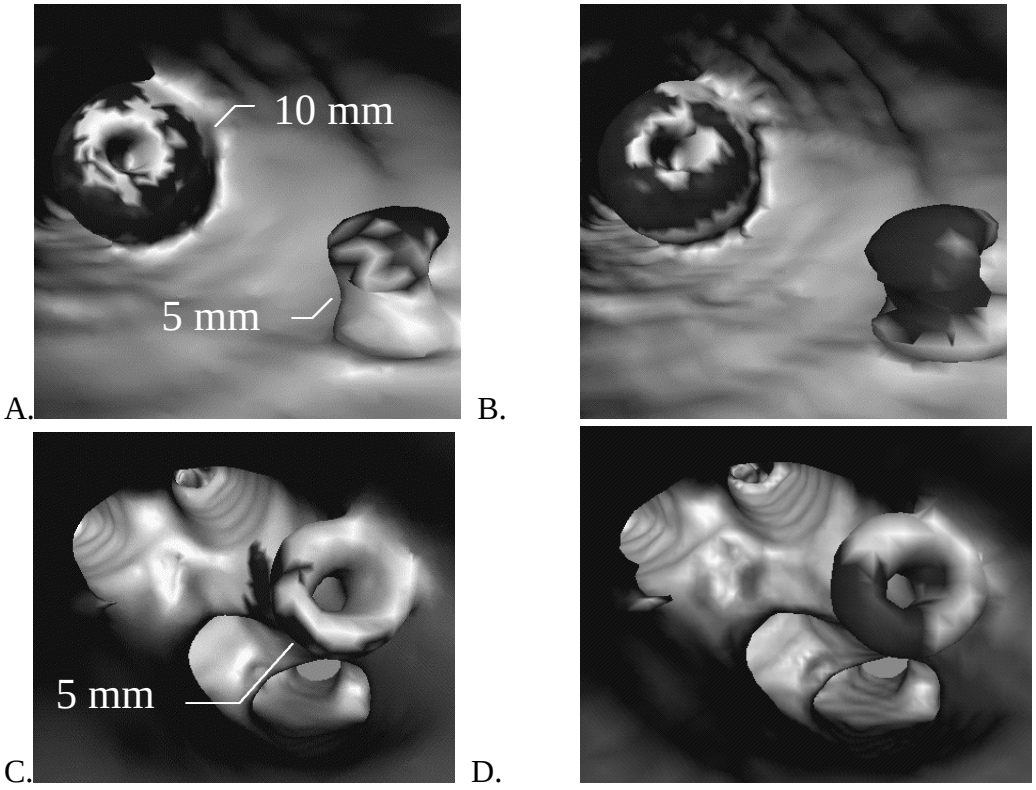

Figure 1. Virtual bronchoscopy of a latex phantom of the central airways. Simulated endobronchial lesions (spherical beads) were affixed to the wall of the phantom. Automatic lesion detection was done using patch (A, C) and grey-scale (B, D) methods. A, B. View of two simulated lesions 10 and 5 mm in diameter (arrows) within a mainstem bronchus. (C, D) View of a 5 mm diameter lesion (arrow) in the distal left lower lobe bronchus. For the grey-scale method, the kernel size was 11x11x11. Note that margins of "lesions" in B and D are smoother and there are no areas of drop-out within the lesion (indicating more homogeneous detection). For the 10 mm lesion, the detected region is larger using the patch method. For the 5 mm lesion, the detected region is larger using the grey-scale method. This is because the grey-scale method tends to be less sensitive for areas of lower curvature and the patch method is less sensitive for areas of greater curvature.

A.

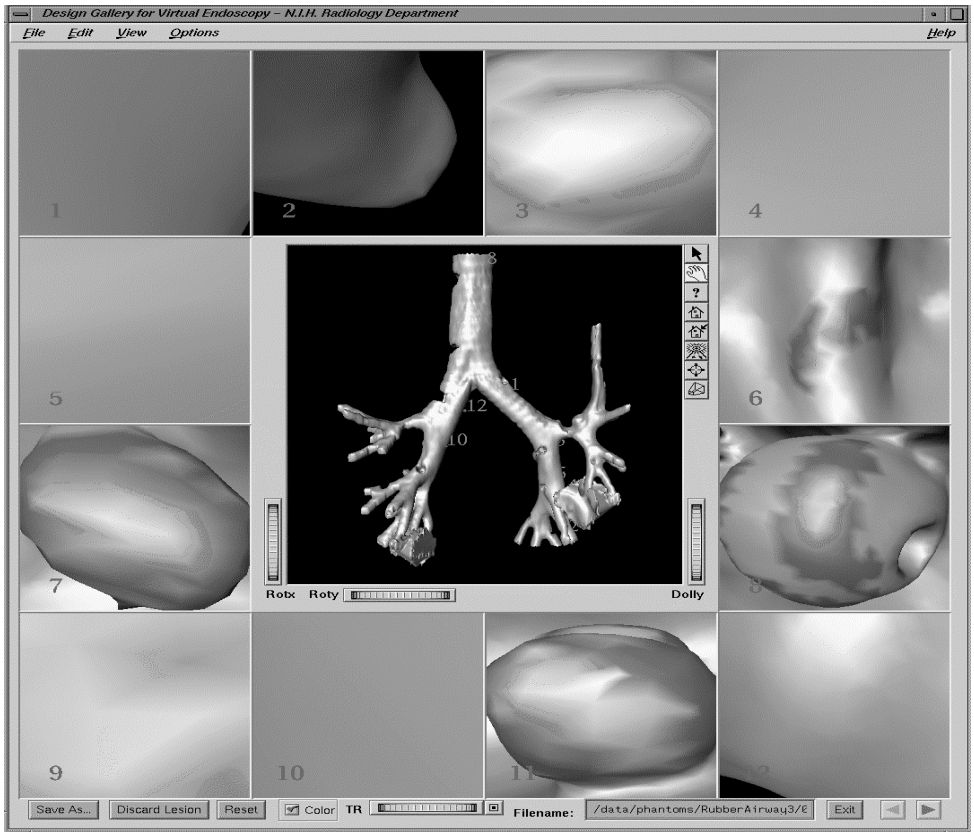
Design Gallery for Virtual Endoscopy – N.I.H. Radiology Department
File
Edit
View
Options
Help
Rotx
Roty
Dolly
Save As...
Discard Lesion
Reset
Color
TR
Filename:
/data/phantoms/RubberAirway3/
Exit

B.

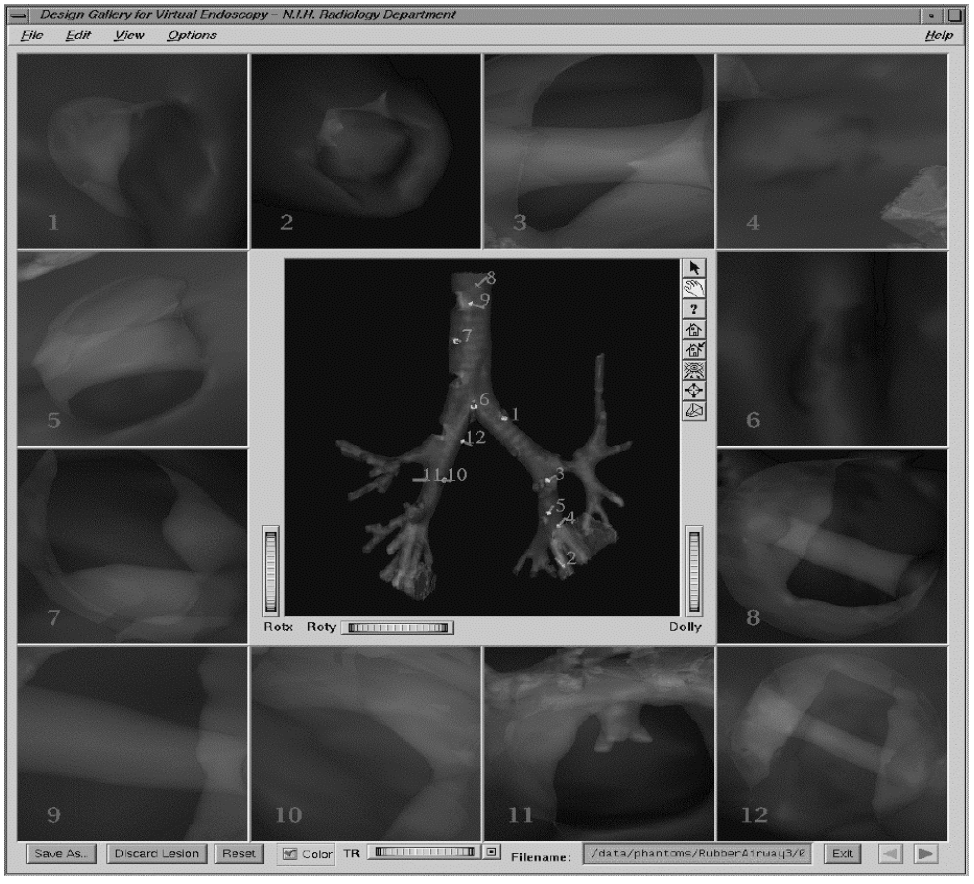
Design Gallery for Virtual Endoscopy – N.I.H. Radiology Department
File
Edit
View
Options
Help
Rotx
Roty
Dolly
Save As...
Discard Lesion
Reset
Color
TR
Filename:
/data/phantoms/RubberAirway3/
Exit

C. 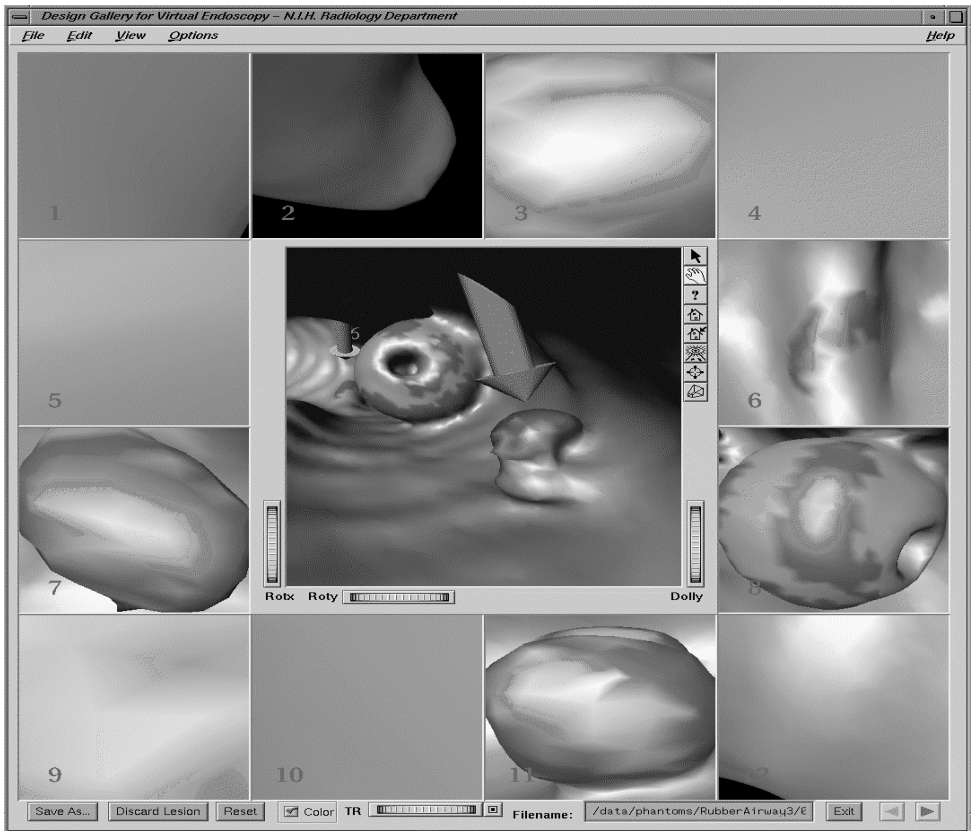

Figure 2. Multiple-window display ("image gallery") showing twelve lesion detections in the airway phantom. The center window shows an "exoscopic" view of the phantom in A and B, and an endoscopic view in C. Twelve candidate lesion sites are shown in an array which frames the central window. Each window represents a separate 3D display and the contents of each window can be manipulated in 3D independently. A. Opaque display. The phantom is rendered opaque. B. Semi-transparent display. The phantom is rendered semi-transparent. The individual lesions inside the phantom are visible. Each lesion detection in the central window is identified with a number and arrow. The number links the lesion to the corresponding endoscopic view in the smaller window in the surrounding frame. C. Virtual bronchoscopy view of two simulated endobronchial lesions. The arrow in the central window which points at a lesion was positioned automatically by the software.

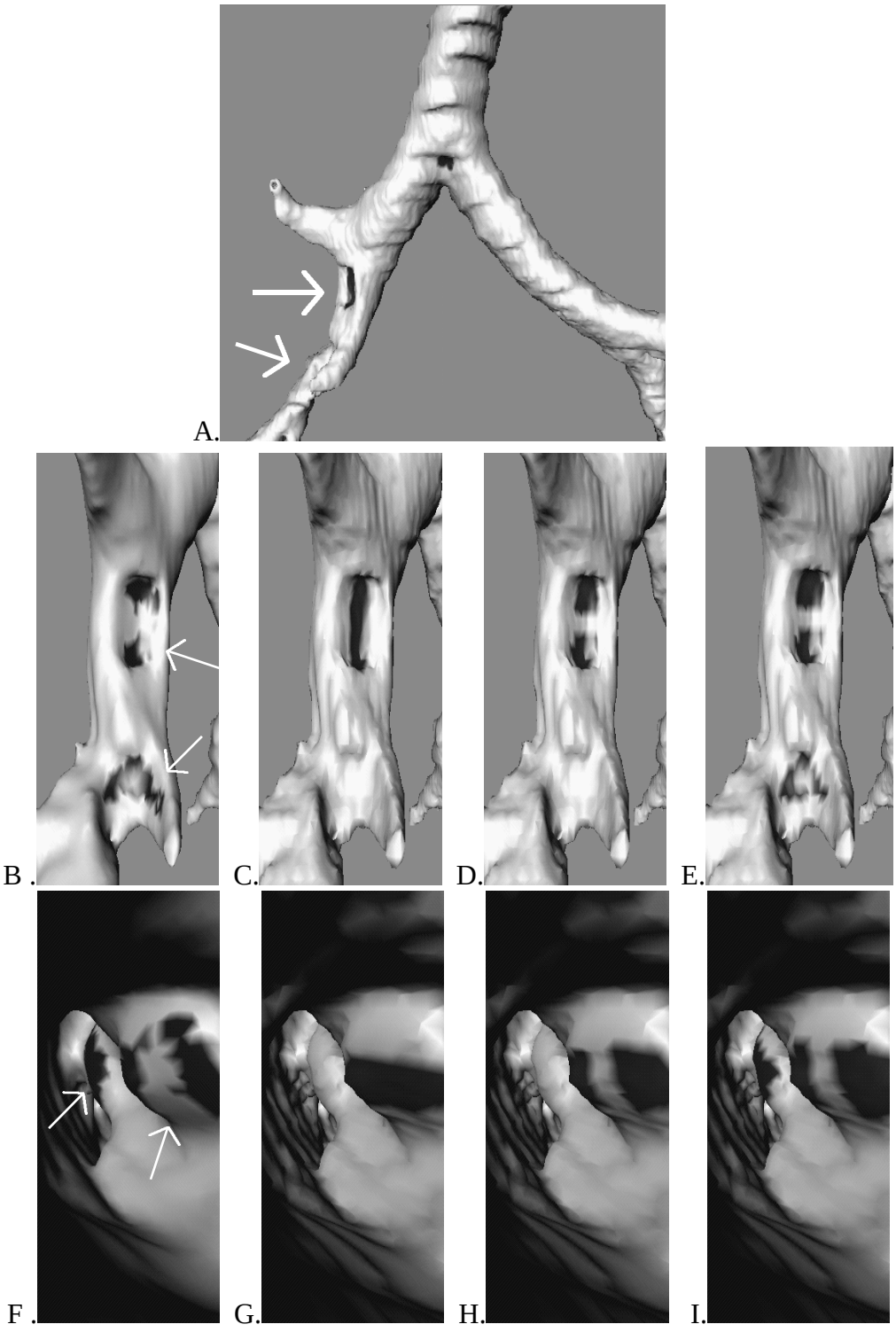

Figure 3. Virtual bronchoscopy of the central airways of a 29 y.o. male patient with melanoma metastatic to the mediastinum and right hilum. A. Frontal exoscopic view of the mainstem carina, mainstem bronchi, and bronchus intermedius. The mass compresses the bronchus intermedius and bifurcation of right middle and lower lobe bronchi (arrows). Right anterior oblique exoscopic views (B-E) and virtual bronchoscopic views (F-I) of the compressed bronchus intermedius. Automatically detected lesion sites are shown in a darker shade, as computed by patch method (B, F), and grey-scale method (C-E, G-I). For the grey-scale method, the kernel sizes were 11x11x11 (C, G), 9x9x9 (D, H), and 7x7x9 (E, I), voxels. In the virtual bronchoscopy, the viewpoint is within the bronchus intermedius looking distally towards right lower lobe bronchus. Note that margins of "lesion" in E and I are slightly smoother and that inferior component of bronchial narrowing is detected by grey-scale method only when a small kernel is used.